LUPINE PUBLISHERS

An archive of organic and inorganic chemical sciences

DOI: 10.32474/AOICS.2020.04.000193

ISSN: 2637-4609

Short Communication

The Washing Effect of Quaternary Layered NCMA Cathode Materials

Xiang Zhangb[2], Yang Shib, Shiguo Xua[1]*, Xiaoyan Zhoua[1], Kaihua Xub[2]*, Yujun Zhanga[1]*, Wei Lia[1]*, Ningjing Liao[1], Haibo wangcde[3,4,5], Jianqing Zhao[3,4]

[1]*GEM new energy materials research institute, GEM (Wuxi) energy material CO, China*

[2]*GEM CO., LTD, Shenzhen, 518101, China*

[3]*Soochow Institute for Energy and Materials Innovation, School of Energy, Soochow University,China*

[4]*Jiangsu Provincial Key Laboratory for Advanced Carbon Materials and Wearable Energy Technologies, Soochow University, China*

[5]*Institute of Chemical Power Sources, Soochow University, China*

***Corresponding author:** Shiguo Xua,GEM new energy materials research institute, GEM (Wuxi) energy material CO., LTD, Wuxi, 214142, China

Received: June 27, 2020 **Published:** August 10, 2020

Abstract

$Li(Ni_{0.82}Co_{0.11}Mn_{0.05}Al_{0.01})O_2$ (NCMA) cathodes are synthesized by adding Al_2O_3 during high temperature solid state reaction. The results show that Al element can largely increase the surface stability of cathode compared to pristine NCM cathode and thus suppress the severe capacity fading after washing process. NCMA delivers a discharge capacity of 203.8 mAh g^{-1} at 0.2 C, with an outstanding capacity retention of 94% after 50 cycles at 25°C. This proposed synthesis strategy demonstrates that an optimal doping method will immensely retain the electrochemical performance while reduce content of the residual lithium compounds during the washing process which promote industrial fabrication of cathode materials.

Keywords: NCMA; washing process; cathode material; Li-ion battery Abbreviations: $Li(Ni_{0.82}Co_{0.11}Mn_{0.05}Al_{0.01})O_2$ (NCMA); $Li(Ni_{0.83}Co_{0.12}Mn_{0.05})O_2$ (NCM); Scanning electron microscope (SEM); X-ray diffraction spectra (XRD); Cyclic voltammetry (CV); Electrochemical impedance spectroscopy (EIS)

Introduction

Lithium-ion batteries (LIBs) have been widely studied to meet the growing demand for the portable electronic devices and electrical vehicles [1, 2]. The $LiNixCoyMnzO_2$ cathode materials (NCM) are considered to be the most promising cathode materials due to the high specific capacity and low capital cost [3, 4].Notably, the specific capacity of NCM can be improved by increasing the Ni composition in the layered structure. However, the Ni-rich cathodes with nickel content above 80% suffer from poor surface stability which hindered the practical application of the Ni-rich cathode materials [5-8].

Compared to NCM523, NCM811 is more susceptible to atmosphere as NCM811 is a fairly hygroscopic material [9]. The residual lithium compounds such as LiOH and Li_2CO_3 originate from spontaneous surface reduction with moisture and air are strongly related to the safety issue and battery performance [10-14]. Li_2CO_3 is responsible for the gas generation which may be arise from the decomposition reaction with electrolytes when charged to high voltage (>4.1V) in the cell [15-17]. On the other hand, LiOH will increase the pH value thus causing the gelation of the slurry during the electrode fabrication process [3]. Hence, the washing process was adapted to remove the residual lithium compounds of Ni-rich cathode. Although washing process greatly reduce the residual lithium compounds and pH value, the direct contact with water will facilitates the phase transition from the layered structure to the NiO like structure which shows no electrochemical activity [18]. The

degradation of surface is fatal to the electrochemical performance and practical application of Ni-rich cathodes [19-21].

Recently, Kim et al. report the quaternary layered Ni-Rich cathode which maintain the specific capacity and excellent cycling stability [22, 23]. In addition to the suppression effect of Al-doping during the H_2-H_3 phase transition, the substitution of Al element greatly reinforces the surface of cathode. However, quaternary layered Ni-Rich cathode still suffer from residual lithium compounds and few paper shows the battery performance of the NCMA cathode materials before and after washing process. In this paper, we report on the structure and electrochemical properties of NCMA and NCM before and after washing process by SEM, XRD, CV, EIS and galvanostatic cycle analysis.

Experimental Method

Materials Synthesis

The NCMA quaternary layered materials were synthesized by the solid-state method using LiOH (Ganfeng Lithium Co. Ltd), transition-mental hydroxide precursors $Ni_{0.83}Co_{0.12}Mn_{0.05}(OH)_2$ (GEM Co. Ltd.) as raw materials and a trance amount of Al_2O_3 (Sigma) was added as doping additive. The $Ni_{0.83}Co_{0.12}Mn_{0.05}(OH)_2$ precursor was mixed thoroughly with LiOH (Li:Ni+Co+Mn=1.02:1) and Al_2O_3 and then the mixture was calcined at 800℃ for 12h in oxygen. For comparison, the NCM cathode materials were synthesized by mixing LiOH and $Ni_{0.83}Co_{0.12}Mn_{0.05}(OH)_2$ precursor (Li:Ni+Co+Mn=1.02:1) and then calcined at 800℃ for12 h in oxygen.

The positive electrode material after sintering and crushing was mixed with purified water in a mass ratio of 1:1 and then stirred for 5 min. The materials were collected through filtering and finally dried at 120℃ in a vacuum oven, which were recorded as NCMA-WD and NCM-WD, respectively.

Materials characterizations

The surface morphologies of the cathode materials were observed with the FEG250 scanning electron microscope produced by FEI Company. The test voltage was 5-15kv and the working distance was 10-11 mm. The phase and crystal structure of the materials were characterized by the XRD-7000 X ray diffractometer produced by Japan shimon using Cu-Ka radiation at 40kV. The scanning speed was 2°/min, and the 2 theta Angle was 15-75°.

The X-ray Rietveld refinement was performed by the General Structure Analysis Software (GSAS) package with the EXPGUI interface. The refining parameters included background coefficients, lattice parameters, peak shape parameters, the positional parameter of O (6c), the fractional factors of all Li, Ni, Co, Mn and Al [24-26].

Electrochemical measurement

Electrochemical properties of the cathode materials were evaluated using CR2032 coin-type half-cells. The prepared cathode materials were mixed with conductive carbon and polyvinylidene fluoride with a mass ratio of 80:10:10. Then all above materials were dissolved in N-methyl pyrrolidone solvent (NMP) and mixed uniformly using a ball mill. After mixing evenly, the uniform slurries were coated on the aluminum foil and dried at 120℃. Then the coated aluminum foil was punched into pellets with a diameter of 13 mm and dried in a vacuum oven for 8 h. Then the CR2032 coin-type half-cells were assembled in the order of battery shell (buttom), negative plate (lithium wafer), diaphragm, electrolyte, positive plate, reed, and battery shell (up) in a glovebox under argon atmosphere. The active mass loading was about 9 mg/cm^2. The electrolyte was 1.0 M LiPF6 dissolved in a mixture of ethylene carbonate (EC), dimethyl carbonate (DMC), ethyl methyl carbonate (EMC) with the volume ratio of 1:1:1. The Discharge-charge tests were performed at the charge or discharge ratio of 0.5C on a LAND battery test system produced by Wuhan blue electric company. Cyclic voltammetry and AC impedance tests were carried out by the electrochemical workstation Solartron (1287+1260) with the scanning speed of 0.1 mV/s and voltage range from 3.1 V to 4.5 V for cyclic voltammograms test. The frequency range of AC impedance test was 0.01 Hz–105 Hz, and AC amplitude was 100 mV.

Results and discussion

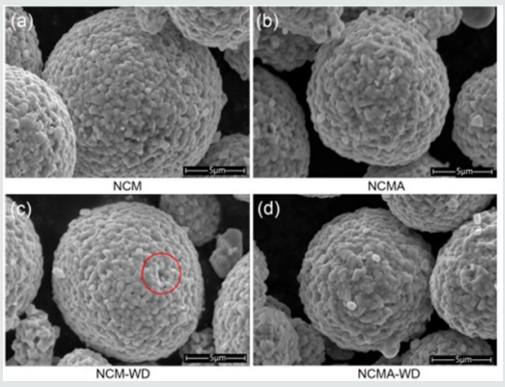

Figure 1: SEM images of NCM, NCMA, NCM-WD and NCMA-WD.

Figure 1 shows the SEM images of pristine and washed powders of NCM and NCMA cathode materials. All of the powders display a spherical morphology and each spherical secondary particle is composed of an agglomerate of primary particles. The exquisite observation on the NCMA surface shows that edges and corners of particles became obscure and the primary particle size distributes larger compared to the pristine NCM which indicates more interact between the primary particles. In addition, the primary particles were found removed during the washing process as is marked in Figure 1c while no obvious defects were detected in NCMA powders. This implies that introducing of Al element into the NCM materials improves the spatially correlation of primary particles.

Figure 2 shows the X-ray powder diffraction patterns of the samples. All of the samples exhibit a well-defined layer structure based on a hexagonal α-$NaFeO_2$ structure with a R-3m space group without any impurity phases [27]. The clear peak splits of the (006)/(102) and (018)/(110) peaks are observed for all samples, indicating that all the samples have well-defined layered structures [28]. Rietveld refinement results shows that the Al element decrease the Li/Ni exchange from 1.9% (NCM) to 1.6% (NCMA).

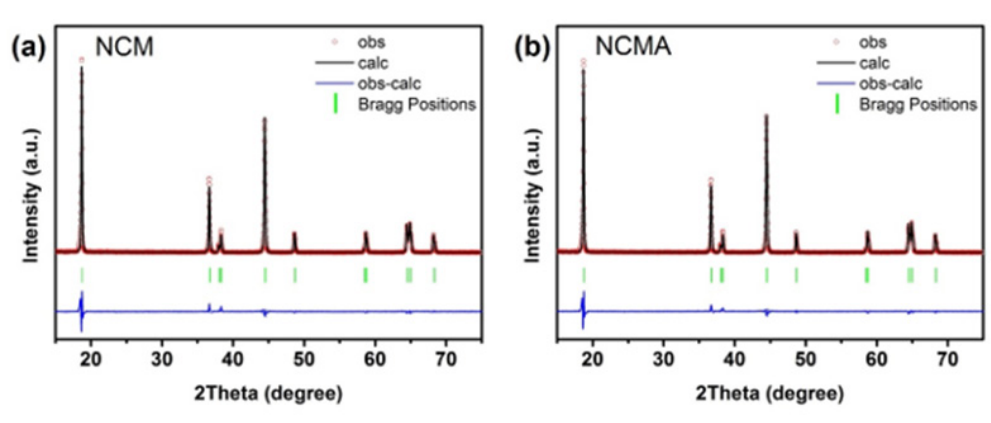

Figure 2: Powder XRD patterns of the NCM and NCMA.

Figure 3 shows the cyclic voltammetry analysis of all materials between 3.1 and 4.5 V (vs. Li/Li^+) at a scan rate of 0.1 mV s^{-1} in the first cycle. It can be seen that the four materials have similar redox peaks at 4.16V/4.22V, which corresponds to the platform near 4.20V on the charge-discharge curve and represents the transformation between H2 and H3 of the hexagonal crystal phase. The redox peak at 3.71V/4.06V corresponds to the redox process of Ni^{2+}/Ni^{4+} [29-31]. Tiny cathodic peaks P0 and P4 are observed at around 3.50V and then disappear in the subsequent oxidation process, which may be attributed to the irreversible decomposition of impurities at the electrode/electrolyte interface as no relative cathodic peaks are detected in the washed samples. As shown in the cyclic voltammetry curves, the overpotential between first redox peaks (ΔV) of NCM and NCMA are 0.350 V and 0.345 V, while the ΔV of NCM-WD and NCMA-WD are 0.353 V and 0.323V, respectively. The washing process decrease ΔV of NCMA-WD by 0.02 V, which indicates that the washing process will remove the residual lithium compounds on the material and increase the reversibility and reactivity of the cathode material. On the other hand, NCM-WD shows larger overpotential than NCMA-WD which should be attributed to the stable effect of Al doping on the structure. CV curves present that the Al doping modify the surface of the powders and suppress the destruction of water.

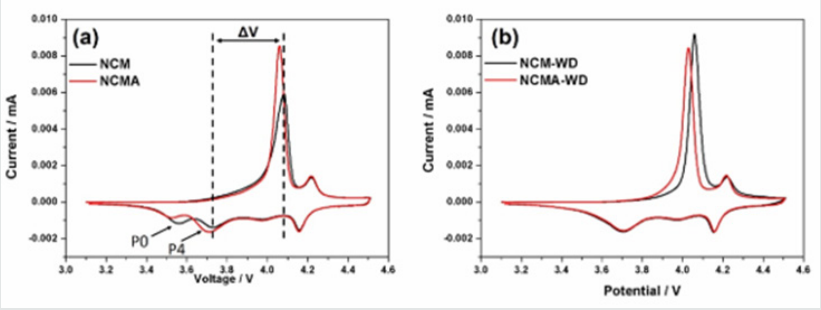

Figure 3: Cyclic voltammetry curves of all materials.

Figure 4 shows the initial charge-discharge curves for the four materials tested at 0.2 C. There is no significant difference between the initial discharge capacities of NCM and NCMA of approximately 192 mAh g^{-1}. However, NCM-WD and NCMA-WD show larger initial discharge capacity of 200.4 and 203.8 mAh g^{-1} which may be arise from the removing of impurity on the surface by washing process.

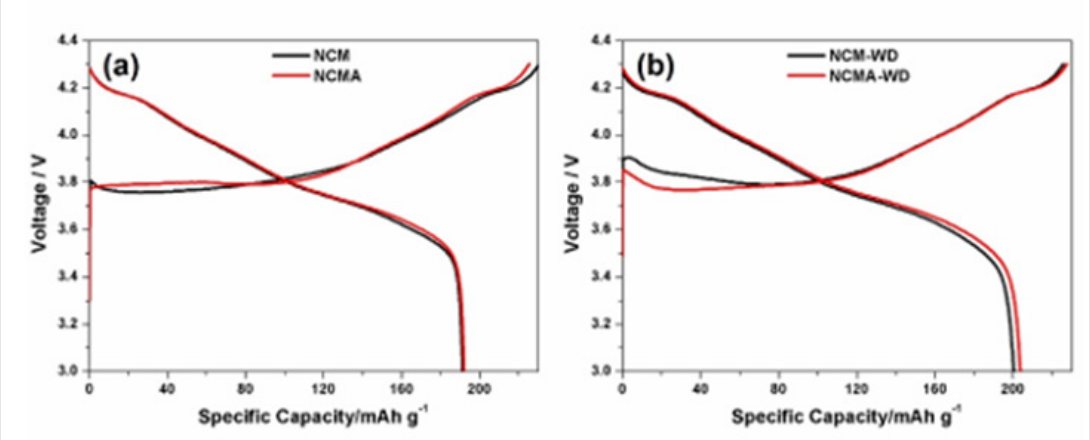

Figure 4: Charge-discharge curves of NCM and NCMA (a); NCM-WD and NCMA-WD (b).

Figure 5 shows the cycle performances of all the materials, NCMA shows similar capacity retention with NCM while NCMA-WD shows greatly improved capacity retention compared with NCM-WD. It should be noted that after washing process, both NCM-WD and NCMA-WD show superior capacity which may be arise from the remove of residual lithium compounds but the poor capacity retention of NCM-WD is derived from the structural instability of the material after washing process.

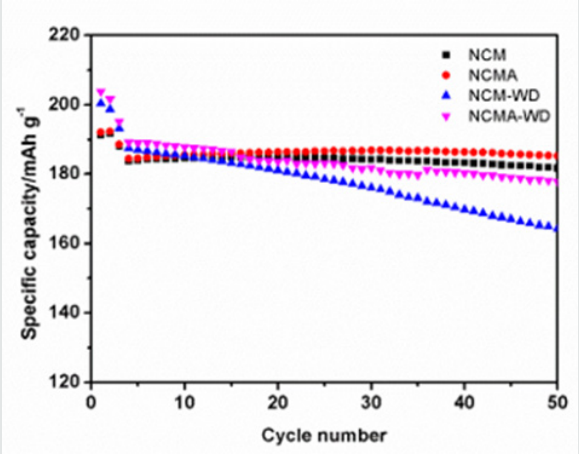

Figure 5: Cycling performances of NCM, NCMA, NCM-WD and NCMA-WD.

EIS spectra of samples has been measured after 1 cycle and 50 cycles as shown in Figure 6. The plots consist of two semicircles in the high frequency region. The semicircle at high frequency could be attributed to the resistance for Li ion migration through surface film (RSEI) and semicircle at high-to-medium frequency is assigned to the surface charge transfer process (Rct). The cathodes show similar surface film resistances, but the charge-transfer resistance, Rct, differed substantially depending on the treating process. The Rct value increased appreciably from the surface decomposition during washing process. Al element dramatically decrease the Rct which should be assigned to the surface stabilization of the Al element. In addition, the value for Rct of NCM gradually accumulated after 50 cycling and obviously vary from the NCMA although they have similar Rct after 1 cycle. As shown in Figure 5, NCMA-WD maintain the excellent ability of Li conduction after washing process while NCM-WD after 50 cycles shows tremendous Rct value compared with that of the pristine material for the structural degradation of surface during washing process.

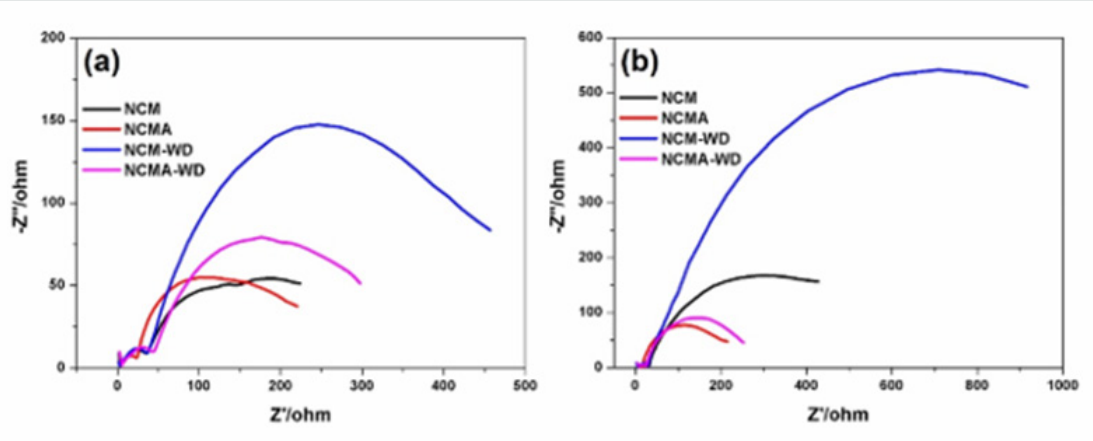

Figure 6: Nyquist plots of all materials after 1cycle (a) and 50 cycles (b).

Conclusion

We synthesized NCMA cathodes by high-temperature solid state method. The partial substitution of Ni with Al element can facilitate the growth of primary particles and improve the spatially correlation of primary particles which reduce the destruction of secondary particles during washing process. Optimal Al-doping reduce the overpotential of the cathode and retain the capacity of the material. Moreover, the EIS analysis shows that the Al-doping can retard structural degradation of surface and maintain the capacity retention during washing process. The NCMA cathode after washing process delivers a discharge capacity of 203.8 mAh g^{-1} at 0.2 C with an outstanding capacity retention of 94% after 50 cycles at 25°C. This proposed synthesis strategy demonstrates that an optimal doping method will immensely retain the electrochemical performance while reduce content of the residual lithium compounds during the washing process which promote industrial fabrication of cathode materials.

Declarations of Interest

The authors declare no competing financial interest.

Acknowledgements

This work was supported by Industrialization Project of Wuxi (WX18IVHC719).

References

1. Armand M, Tarascon JM (2008) Building better batteries, Nature: 451: 652-657.
2. Dunn B, Kamath H, Tarascon JM (2011) Electrical energy storage for the grid: a battery of choices. Science 334: 928-935.
3. Liu W, Oh P, Liu X, Lee MJ, Cho W, and et al., (2015) Nickel-Rich Layered Lithium Transition-Metal Oxide for High-Energy Lithium-Ion Batteries. Angew Chem Int 54: 4440-4457.
4. Thackeray MM, Wolverton C, Isaacs ED (2012) Electrical energy storage for transportation-approaching the limits of, and going beyond, lithium-ion batteries. Energy Environ Sci 5: 7854.
5. Manthiram A, Knight JC, Myung ST, Oh SM, Sun YK (2016) Nickel-Rich and Lithium-Rich Layered Oxide Cathodes: Progress and Perspectives. Adv Energy Mater 6: 1501010.
6. Kim J, Lee H, Cha H, Yoon M, Park M, and et al., (2018) Prospect and Reality of Ni-Rich Cathode for Commercialization. Adv Energy Mater 8: 1702028.
7. HJ Noh, Youn S, Yoon CS, Sun YK (2013) Comparison of the structural and electrochemical properties of layered $Li[Ni_xCo_yMn_z]O_2$ (x=1/3, 0.5, 0.6, 0.7, 0.8 and 0.85) cathode material for lithium-ion batteries. J Power Sources 233: 121-130.
8. Li W, Liu X, Celio H, Smith P, Dolocan A and et al., (2018) Mn versus Al in Layered Oxide Cathodes in Lithium-Ion Batteries: A Comprehensive Evaluation on Long-Term Cyclability. Adv Energy Mater 8(15): 1703154.
9. Lin Y, Xu M, Tian Y, Fan W, Yu L, and et al., (2018) Understanding impacts of environmental relative humidity to the cell performance based on $LiNi_{0.8}Co_0.15Al_{0.05}O_2$ cathode. Mater Chem and Phys 211: 200-205.
10. Aurbach D (1995) The Study of Electrolyte Solutions Based on Ethylene and Diethyl Carbonates for Rechargeable Li Batteries. J Electrochem Soc 142: 2873.
11. Liu H, Yang Y, Zhang J (2007) Reaction mechanism and kinetics of lithium ion battery cathode material $LiNiO_2$ with CO_2. J Power Sources 173(1): 556-561.
12. Cho DH, Jo CH, Cho W, Kim YJ, Yashiro H, and et al., (2014) Effect of Residual Lithium Compounds on Layer Ni-Rich $Li[Ni_{0.7}Mn_{0.3}]O_2$. J The Electrochem Soc 161(6): A920-A926.
13. Tasaki K, Goldberg A, Lian JJ, Walker M, Timmons A, and et al., (2009) Solubility of Lithium Salts Formed on the Lithium-Ion Battery Negative Electrode Surface in Organic Solvents. J Electrochem Soc 156: A1019.
14. Zhuang GV, Chen G, Shim J, Song X, Ross PN, and et al., (2004) Li_2CO_3 in $LiNi_{0.8}Co_{0.15}Al_{0.05}O_2$ cathodes and its effects on capacity and power. J Power Sources 134(2): 293-297.
15. Robert R, Bünzli C, Berg EJ, Novák P (2015) Activation Mechanism of $LiNi_{0.80}Co_{0.15}Al_{0.05}O_2$: Surface and Bulk Operando Electrochemical, Differential Electrochemical Mass Spectrometry, and X-ray Diffraction Analyses. Chem Mater 27: 526-536.
16. Rahman MK, Saito Y (2007) Investigation of positive electrodes after cycle testing of high-power Li-ion battery cells. J Power Sources 1749(2): 889-894.
17. Kim Y (2013) Mechanism of gas evolution from the cathode of lithium-ion batteries at the initial stage of high-temperature storage. J Mater Sci 48: 8547-8551.

18. Zheng S, Huang R, Makimura Y, Ukyo Y, Fisher CAJ, and et al., (2011) Microstructural Changes in $LiNi_{0.80}Co_{0.15}Al_{0.05}O_2$Positive Electrode Material during the First Cycle. J Electrochem Soc 158: A357.

19. Kim J, Hong Y, Ryu KS, Kim MG, Cho J (2006) Washing Effect of a $LiNi_{0.8}Co_{0.15}Al_{0.05}O_2$ Cathode in Water. Electrochem Solid ST 9(1): A19-A23.

20. Xiong X, Wang Z, Yue P, Guo H, Wu F, and et al., (2013) Washing effects on electrochemical performance and storage characteristics of $LiNi_{0.8}Co_{0.1}Mn_{0.1}O_2$ as cathode material for lithium-ion batteries. J Power Sources 222: 318-325.

21. Kim Y (2013) Encapsulation of $LiNi_{0.5}Co_{0.2}Mn_{0.3}O_2$ with a thin inorganic electrolyte film to reduce gas evolution in the application of lithium ion batteries. Physical chemistry chemical physics PCCP 15: 6400-6405.

22. Kim UH, Myung ST, Yoon CS, Sun YK (2017) Extending the Battery Life Using an Al-Doped $Li[Ni_{0.76}Co_{0.09}Mn_{0.15}]O_2$ Cathode with Concentration Gradients for Lithium Ion Batteries. ACS Energy Lett 2: 1848-1854.

23. Kim UH, Kuo LY, Kaghazchi P, Yoon CS, Sun YK (2019) Quaternary Layered Ni-Rich NCMA Cathode for Lithium-Ion Batteries. ACS Energy Lett 4: 576-582.

24. Tang Z, Wang S, Liao J, Wang S, He X, and et al., (2019) Facilitating Lithium-Ion Diffusion in Layered Cathode Materials by Introducing Li^+/Ni^{2+} Antisite Defects for High-Rate Li-Ion Batteries. Research 2019: 2198906.

25. Wang D, Kou R, Ren Y, Sun CJ, Zhao H, and et al., (2017) Synthetic Control of Kinetic Reaction Pathway and Cationic Ordering in High-Ni Layered Oxide Cathodes. Adv Mater 29(39): 1606715-1606723.

26. Wu F, Tian J, Su Y, Wang J, Zhang C, and et al., (2015) Effect of Ni^{2+} content on lithium/nickel disorder for Ni-rich cathode materials. ACS appl Mater inter 7: 7702-7708.

27. Dong M, Wang H Li, Guo, Li X, Shih K, and et al., (2017) Metallurgy Inspired Formation of Homogeneous Al_2O_3 Coating Layer to Improve the Electrochemical Properties of $LiNi_{0.8}Co_{0.1}Mn_{0.1}O_2$ Cathode Material. ACS Sustain Chem Eng 5: 10199-10205.

28. Liu W, Li X, Xiong D, Hao Y, Li J, and et al., (2018) Significantly improving cycling performance of cathodes in lithium ion batteries: The effect of Al_2O_3 and $LiAlO_2$ coatings on $LiNi_{0.6}Co_{0.2}Mn_{0.2}O_2$. Nano Energy 44: 111-120.

29. Jung R, Metzger M, Maglia F, Stinner C, Gasteiger HA (2017) Oxygen Release and Its Effect on the Cycling Stability of $LiNi_xMn_yCoz O_2$(NMC) Cathode Materials for Li-Ion Batteries. J Electrochem Soc 164: A1361-A1377.

30. Qi H, Wenxun Guo, Lingyun Tian, Xiaofeng Wen, Kaiyue Shi, and et al., (2017) Facile Fabrication and Low-cost Coating of $LiNi_{0.8}Co_{0.15}Al_{0.05}O_2$ with Enhanced Electrochemical Performance as Cathode Materials for Lithium-ion Batteries. Int J Electrochem Sci 5836-5844.

31. Huang Z, Wang Z, Zheng X, Guo H, Li X, and et al., (2015) Effect of Mg doping on the structural and electrochemical performance of $LiNi_{0.6}Co_{0.2}Mn_{0.2}O_2$ cathode materials. Electrochim Acta 182: 795-802.

DOI: 10.32474/AOICS.2020.04.000193